



Computational catalysis

Iridium catalyzed hydrogenation of CO₂ under basic conditions—Mechanistic insight from theory[☆]

Mårten S.G. Ahlquist*

Department of Theoretical Chemistry, School of Biotechnology, Royal Institute of Technology, SE-10691 Stockholm, Sweden

ARTICLE INFO

Article history:

Available online 19 February 2010

Keywords:

DFT
Carbon dioxide
Iridium
Catalysis
Hydrogenation
Reduction
Formate
Base
Transition metal
Homogeneous

ABSTRACT

The iridium(III) catalyzed hydrogenation of carbon dioxide under basic conditions was studied with density functional theory. It was found that the insertion of CO₂ into an Ir–H bond proceeds via a two-step mechanism. The rate-limiting step was calculated to be the regeneration of the iridium(III) trihydride intermediate, and the overall barrier for the reaction was calculated to 26.1 kcal mol⁻¹. The formation of the iridium trihydride proceeds via formation of a cationic Ir(H)₂(H₂) complex at which the base abstracts a proton from the dihydrogen ligand.

© 2010 Elsevier B.V. All rights reserved.

1. Introduction

Hydrogenation of carbon dioxide has been proposed as a viable method for storing energy [1,2]. The energy source could be solar radiation used to produce hydrogen from oxidation of water [3,4]. Since the volumetric energy density of hydrogen gas (or even compressed H₂) is low, and since hydrogen gas would require a new distribution network, formation of a liquid fuel from H₂ is desirable. Reduction of CO₂ could in principle yield methanol, which has a high volumetric energy density and which would require only minor modifications to the existing distribution network. However, while methanol would be the most efficient way of storing H₂ from CO₂ reduction it requires three H₂ additions, and it is quite challenging for one catalyst to be capable of performing the reduction of CO₂ and all the intermediates formed in the reaction. The first reduction step to formic acid has been studied by several groups [5,6], and lately an extremely efficient protocol was presented by Nozaki (Scheme 1) [7]. By using an iridium(III) trihydride in aqueous KOH they achieved turnover numbers up to 3.5

million. Herein a theoretical study of the mechanism of a model Ir^{III} catalyst reacting with carbon dioxide and hydrogen is presented.

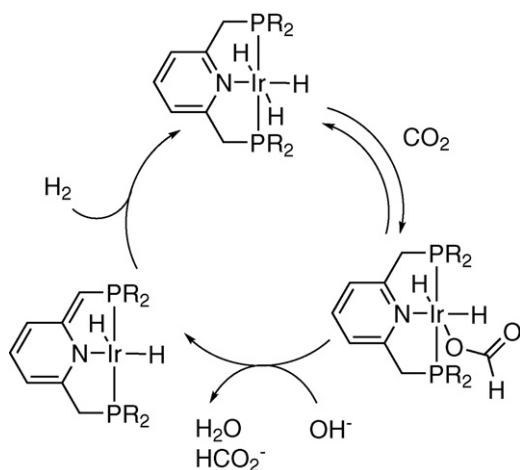
2. Results and discussion

The Ir^{III} trihydride complex **1** was used as the starting point. It was observed experimentally that the trihydride complex was in equilibrium with the formate complex when exposed to CO₂. We calculate the formation of the formate complex **5** to be endergonic by 2.4 kcal mol⁻¹ which is in agreement with the experimental results that the two species are in equilibrium (Scheme 2). The mechanism for the insertion was found to proceed via a two-step process. First CO₂ interacts with one of the axial hydrides to form the H-bound formate intermediate **3** via the transition state **2ts** with a barrier of 14.5 kcal mol⁻¹. The intermediate complex **3** is slightly lower than **2ts** in energy and is at 13.9 kcal mol⁻¹ above **1** and CO₂. Rearrangement to give the O-bound formate was found to pass the highest point on the free energy surface from **1** to **5** and the overall barrier was calculated to 21.9 kcal mol⁻¹. The mechanism is similar to the previously reported extrusion of CO₂ from a palladium(II)–formate complex [8], which first rearranged from the O-bound formate to the H-bound followed by facile CO₂ dissociation. One could also envision the process from **3** to **5** to proceed via dissociation of the formate from **3** followed by reassociation to give the O-bound complex **5**. Since the dissociation of formate from

[☆] This paper is part of a special issue on Computational Catalysis.

* Tel.: +46 8 5537 8415; fax: +46 8 5537 8590.

E-mail address: mahlquist@theochem.kth.se.



Scheme 1. Proposed mechanism by Nozaki.

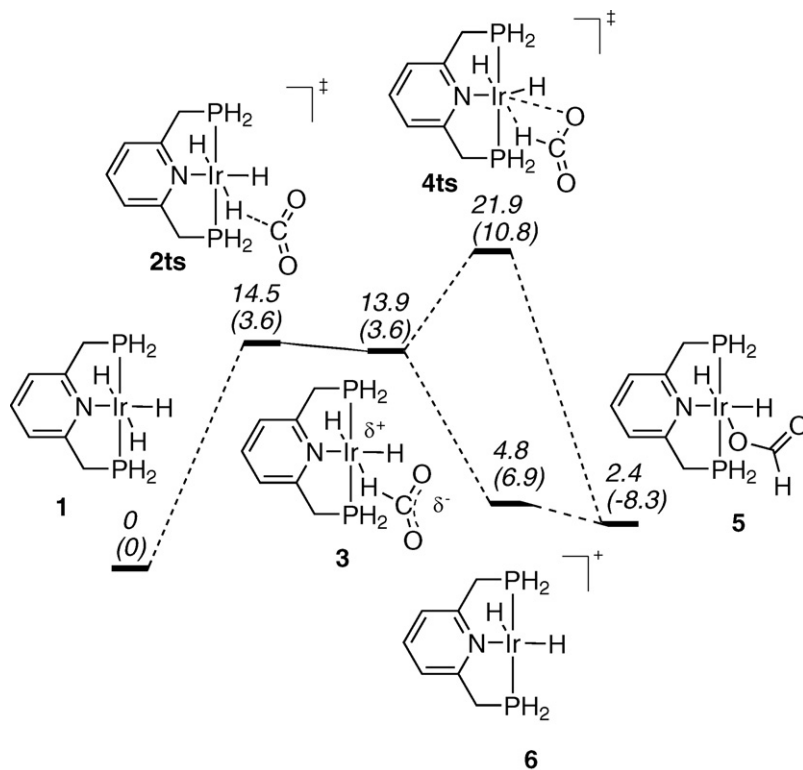
3 to give **6** is exergonic this process is likely the favored path [9] (Fig. 1).

It was proposed that deprotonation of the ligand in the benzylic position would facilitate the dissociation of the formate from **5** [7]. However we find that dissociation of the formate is facile and that the reaction from **5** to **6** is endergonic by merely $2.4 \text{ kcal mol}^{-1}$ (Scheme 3). Under the conditions studied (1 M OH^-) we find that the formation of **10** from **6** where the ligand is dearomatized is unfavorable by $11.3 \text{ kcal mol}^{-1}$. Hydroxide is calculated to bind **6** favorably by $3.0 \text{ kcal mol}^{-1}$ putting complex **7** at $1.8 \text{ kcal mol}^{-1}$ on the free energy surface. The hydroxide complex can transform in to the aquo complex **9** by transferring a proton from the ligand to the hydroxide. The barrier for this process is calculated to $15.7 \text{ kcal mol}^{-1}$. We also note that the geometry of **10** is trigo-

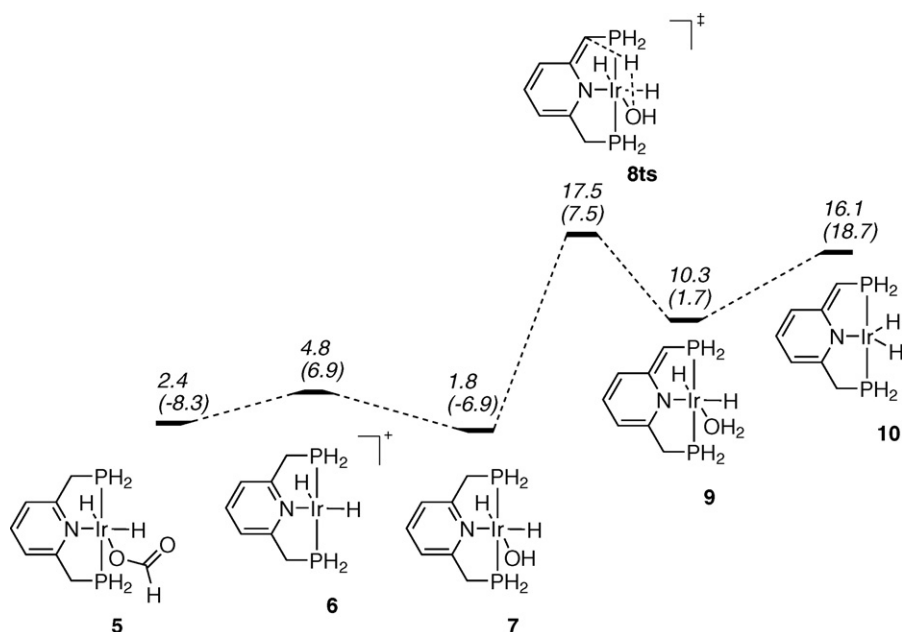
nal bipyramidal, and not square pyramidal. We therefore believe that it could be an octahedral complex similar to **9**, or possibly an anionic complex where the aquo ligand of **9** is deprotonated, which is observed experimentally. In the ^1H NMR spectrum by Nozaki two hydride peaks were observed, which indicates two hydrides in different chemical environment. The deprotonation of **9** is calculated to be favorable by $1.3 \text{ kcal mol}^{-1}$ under the current conditions ($1 \text{ M OH}^-(\text{aq})$). The reaction is likely more exergonic under the experimental conditions where $\text{CsOH}\cdot\text{OH}_2$ was used as the base in THF, since hydroxide (and other non-stabilized anionic alcoxides) is a much stronger base in non-protic solvents than it is in water (pK_a in DMSO = 31.4, pK_a in H_2O = 15.7) [10].

To **6** H_2 can coordinate to give the cationic dihydrogen complex **11** (Scheme 4). Deprotonation by hydroxide (or most favorably $[\text{OH}\cdot\text{OH}_2]^-$) has a barrier of $22.9 \text{ kcal mol}^{-1}$, which puts it at $26.1 \text{ kcal mol}^{-1}$ on the free energy surface. Hence, our calculations suggest that the regeneration of the trihydride complex **1** is the rate-limiting step of the catalysis. Since OH^- is involved in this step an effect of the basicity on the rate is expected, which was also observed experimentally. It is also possible that deprotonation of **6** occurs first to give **10**, followed by homolytic cleavage of H_2 to regenerate **1** directly. The free energy of the transition state for this process was calculated to be at $27.3 \text{ kcal mol}^{-1}$, hence only slightly higher than the deprotonation of the coordinated H_2 (**12ts**). Also for the homolytic cleavage a base effect would be expected since the generation of **10** from **6** involves base.

The generation of **1** from **10** has been studied by Milstein and co-workers previously [11,12], although one of the hydrides in their case was replaced by a phenyl group. They looked at the barrier from the dearomatized complex similar to **10** (with a phenyl group in the equatorial position) and found a transition state similar to **12ts** $6.9 \text{ kcal mol}^{-1}$ above **10**, H_2 , and two water molecules. In our



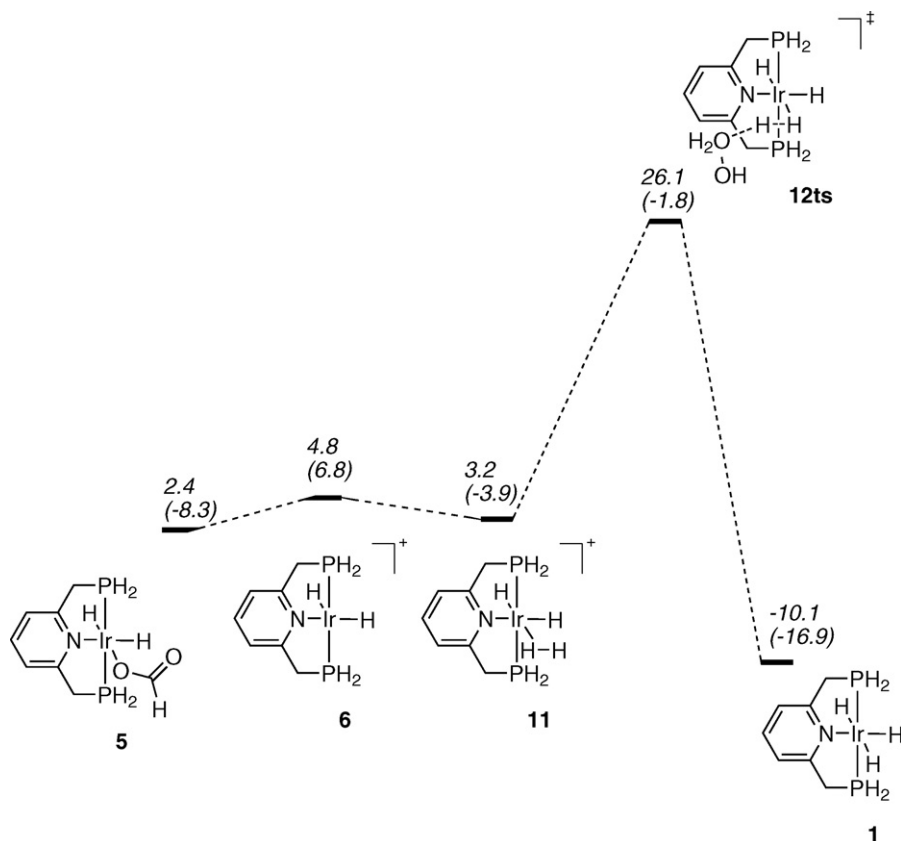
Scheme 2. Calculated reaction path for CO_2 insertion into the Ir–H bond of **1**. Numbers in *italics* relative free energies in kcal mol^{-1} , and in parentheses relative enthalpies in kcal mol^{-1} .



Scheme 3. Relative energies of possible intermediates. Relative free energies in *italics* in kcal mol⁻¹, and in parentheses relative enthalpies in kcal mol⁻¹.

case the barrier is calculated to 9.9 kcal mol⁻¹ for the corresponding step (**10–12ts**), and the result for this reaction step is thus very similar (Scheme 5). We also investigated the possibility of an iridium(I) hydride complex as an intermediate in the catalytic cycle. The formation of the Ir^I-H complex **14** from the dearomatized complex **10** was calculated to be exergonic by 15.1 kcal mol⁻¹, which is slightly more than the 11.1 reported by Milstein yet in the same

range. However, we find a very different reaction barrier. Despite having a geometry very close to the one reported by Milstein, we calculate the reverse rearrangement from **14** to **10** assisted by two water molecules to have a barrier of 34.3 kcal mol⁻¹. This number should be compared to the 20.7 kcal mol⁻¹ barrier previously reported [11]. While the discrepancy could be due to the use of slightly different functionals and basis sets and slightly different



Scheme 4. Calculated reaction path for formation of **1** from **5**. Numbers in *italics* are relative free energies in kcal mol⁻¹, and in parentheses relative enthalpies in kcal mol⁻¹.

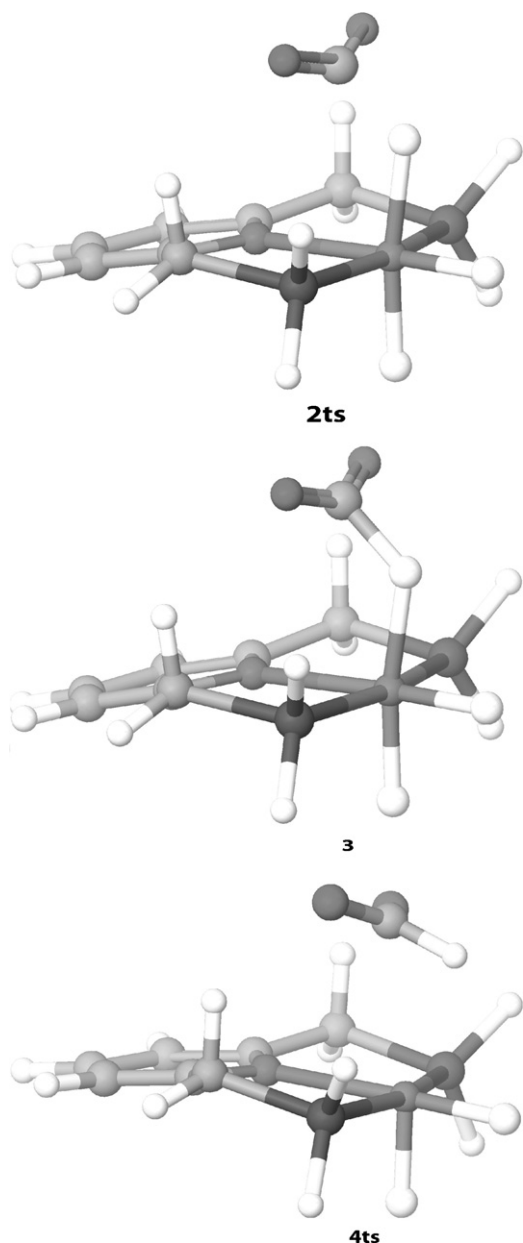


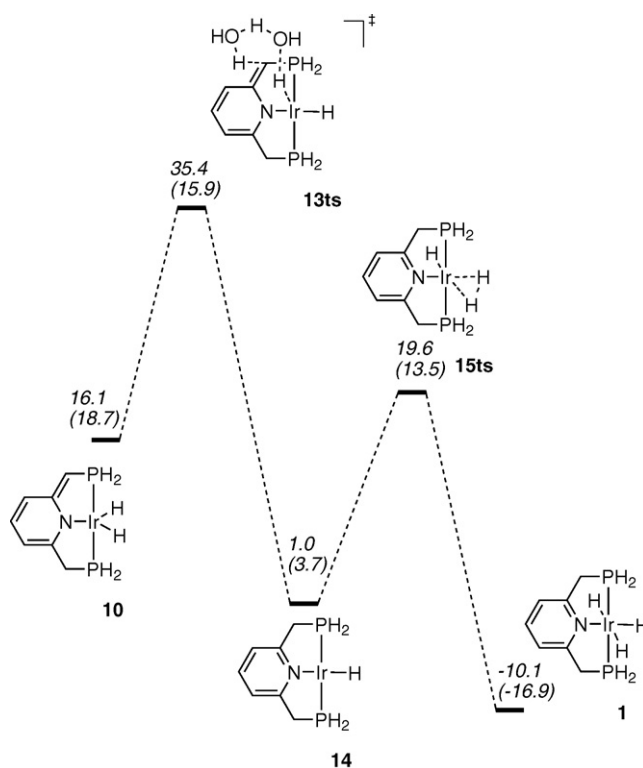
Fig. 1. Geometries of **2ts**, **3**, and **4ts**. Bond distances and angles **2ts** Ir–H¹ 1.76 Å, H¹–C 1.47 Å, C–O¹ 1.21 Å, C–O² 1.21 Å, O–C–O 144°; **3** Ir–H¹ 1.78 Å, H¹–C 1.39 Å, C–O¹ 1.22 Å, C–O² 1.22 Å, O–C–O 142°; **4ts** Ir–H¹ 2.40 Å, H¹–C 1.15 Å, C–O¹ 1.27 Å, C–O² 1.25 Å, Ir–O¹ 2.86 Å, Ir–O² 3.37 Å, O–C–O 131°.

complexes, the difference of almost 14 kcal mol⁻¹ in barrier for the same transformation via transition states with very similar geometry seems a bit too large. More likely the discrepancy stems from different treatment of entropy and solvation. Herein, we have used the values from the Poisson–Boltzmann solver (PBF) in Jaguar 7.5 for the metal complexes while for the small molecules and ions the values in ref 21 have been used. Since we added two explicit water molecules when going from **10** to **13ts** an error could possibly arise if the solvation of water is not correctly described. We therefore added two water molecules to **10** and to **14** (Scheme 6). If the solvation is well described the free energy of going from **10** to **10·2H₂O** and **14** to **14·2H₂O** should be close to zero. We find that ΔG of **10** to **10·2H₂O** is 0.8 kcal mol⁻¹ and **14** to **14·2H₂O** is 0.2 kcal mol⁻¹, which clearly indicates that our description is relatively good. The barrier for **10·2H₂O** to **14·2H₂O** is calculated to 18.5 kcal mol⁻¹ compared to 19.3 kcal mol⁻¹ for **10**–**14**. The bar-

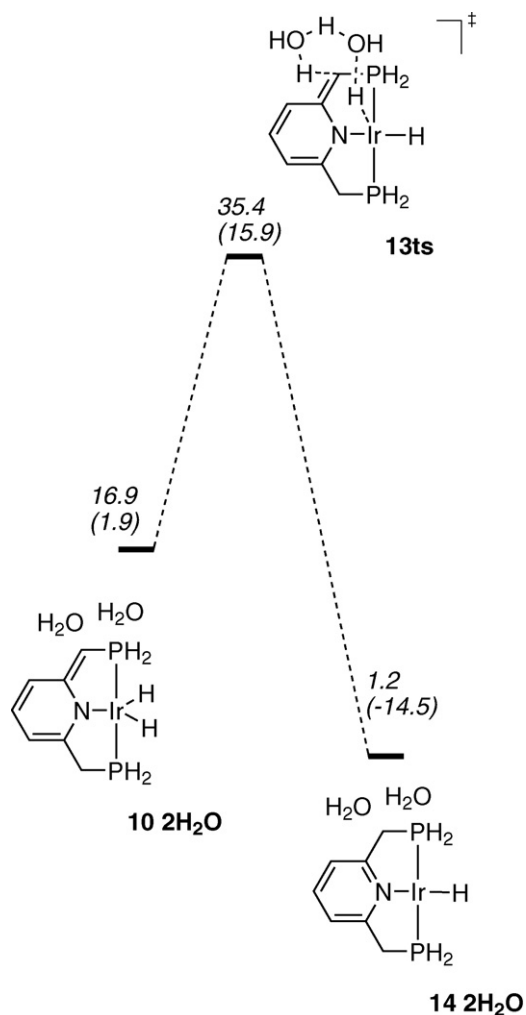
rier for the reverse reaction **14**–**10** differs by merely 0.2 kcal mol⁻¹ when two water molecules are included. These results indicate that the implicit solvent model in the current study works well combined with the experimental solvation energies for water. We note that the free energy for including two explicit water molecules to the iridium(I) complex similar to **14** reported by Milstein was negative by -6.7 kcal mol⁻¹, which indicates erroneous treatment of the solvent.

On our free energy surface the proton transfer transition state **13ts** is at 35.4 kcal mol⁻¹, which make it inaccessible and despite the relatively high stability of the iridium(I) complex **14** the involvement of **14** in the catalytic cycle seems unlikely, unless there is another unknown process for conversion of **10** to **14**. If such an unknown path is present **14** could very well take part in the mechanism. The oxidative addition of H₂ to give **1** is calculated to have a barrier of only 18.6 kcal mol⁻¹ which puts it at 19.6 kcal mol⁻¹ on the free energy surface. We propose that an improved protocol could be found if the formation of **14** is facilitated.

Interestingly, we note that all the intermediates on the free energy surface we propose to form after **1** (**3**, **5**, **6**, and **11**) are all slightly above **1**, with **3** being the highest at 13.9 kcal mol⁻¹. This observation is important since it gives a clue on how to design an efficient catalyst. Since the overall free energy of the reaction is calculated to -10.1 kcal mol⁻¹ any intermediate before the regeneration of **1** lower than that would be detrimental to the catalysis. Hence, when investigating a new catalyst we propose that one first locates all plausible intermediates and if one is too low in energy the catalyst is likely not a good candidate. One could also look at the effect of additives such as halogen ions, or different bases. If these bind too strongly to an intermediate such as **6**, these will likely have a negative impact on the catalytic activity.



Scheme 5. Conversion of **10** to the Ir^I complex **14** and subsequent oxidative addition of H₂. Numbers in *italics* are relative free energies in kcal mol⁻¹, and in parentheses relative enthalpies in kcal mol⁻¹.



Scheme 6. Conversion of $10 \cdot 2\text{H}_2\text{O}$ to the Ir^{I} complex $14 \cdot 2\text{H}_2\text{O}$. Numbers in *italics* are relative free energies in kcal mol^{-1} , and in parentheses relative enthalpies in kcal mol^{-1} .

3. Conclusions

The mechanism of the iridium(III) trihydride complex **1** has been studied by density functional theory. We found that the formate complex **5** is formed via a two-step process. First an H-bound formate complex is formed which rearranges into the more stable O-bound complex. We believe that the rearrangement from the H-bound complex **3** to the O-bound **5** could proceed via dissociation and reassociation. Next the formate dissociates and is replaced by a hydrogen molecule which coordinates to the iridium(III) center. Deprotonation by an hydroxide regenerates the active iridium(III) trihydride. The deprotonation is calculated to be the rate-limiting step and thus agrees with the experiments that higher basicity leads to higher rates.

Regarding the proposed dihydride intermediate **10** where the ligand is dearomatized, our results suggest that the experimentally observed complex could be another one. We propose that the geometry is octahedral with either a neutral or an anionic ligand in the axial position.

The iridium(I) hydride **14** was found to be thermodynamically accessible and very reactive towards dihydrogen with a barrier of only $18.6 \text{ kcal mol}^{-1}$. However, the lowest energy transition state located for the formation of **14** was found to be at 35.4 on the free energy surface, hence making **14** kinetically inaccessible.

4. Computational details

All calculations were performed using the B3LYP [13,14] flavor of density functional theory as implemented in Jaguar 7.5 [15], except the final energy corrections, which were performed with M06 [16]. For geometry optimizations, solvation energy and frequency calculations the LACVP** core potential and basis set was used, while for single point energy corrections LACV3P**++ augmented with two *f*-functions on Ir as suggested by Martin was used [17,18]. All geometries were optimized in the gas phase and single point solvation energies were calculated with the Poisson–Boltzmann self-consistent reaction field (PBF) in Jaguar [19,20]. The dielectric constant was set to 80.37 and the probe radius to 1.40 to simulate water. For water, hydroxide and formate the solvation free energies from Cramer and Truhlar were used [21]. The Jaguar solvent model has been shown to be quite accurate for solvation of larger ionic species and reproduce experimental data well [22,23]. Smaller ions however are known to give larger errors likely due to the incapability of charge transfer from the molecule to the solvent. Using experimental solvation energies for the smaller molecules and ions has been shown previously to give accurate energies for ligand exchange thermodynamics and barriers at palladium complexes [24]. While it is possible that the solvent model does not give accurate absolute solvation energies of the metal complexes the results by Goddard indicates that the relative energies are good. All transition states were confirmed to be first-order saddle points by analytical frequency calculations. The Gibbs free energies were calculated as the sum $G = E(\text{M06/LACV3P}^{**++}(2f)) + G_{\text{solv}} + \text{ZPE} + \Delta H^{298} + S^{298}$, and enthalpies were calculated as the sum $H = E(\text{M06/LACV3P}^{**++}(2f)) + G_{\text{solv}} + \text{ZPE} + \Delta H^{298}$. To solution phase species $1.9 \text{ kcal mol}^{-1}$ was added to the free energy to correct for the change of standard state from 1 atm to 1 M. We note that the enthalpies include some entropic contribution in the G_{solv} term, and when explicit solvent molecules are included the relative enthalpies appears to be low. However, when the explicit solvents are included in reactants, products, and transition states the enthalpies make more sense, as in the case $10 \cdot 2\text{H}_2\text{O} \rightarrow 13\text{ts} \rightarrow 14 \cdot 2\text{H}_2\text{O}$.

Acknowledgement

The author acknowledges the Knut and Alice Wallenberg foundation for financial support.

Appendix A. Supplementary data

Supplementary data associated with this article can be found, in the online version, at [doi:10.1016/j.molcata.2010.02.018](https://doi.org/10.1016/j.molcata.2010.02.018).

References

- [1] G.A. Olah, A. Goepfert, G.K. Surya Prakash, *J. Org. Chem.* 74 (2009) 487–498.
- [2] M. Rakowski Dubois, D.L. Dubois, *Acc. Chem. Res.* 42 (2009) 1974–1982.
- [3] D. Nocera, *Chem. Soc. Rev.* 38 (2009) 13–15.
- [4] D. Gust, T.A. Moore, A.L. Moore, *Acc. Chem. Res.* 42 (2009) 1890–1898.
- [5] W. Leitner, *Angew. Chem. Int. Ed.* 34 (1995) 2207–2221.
- [6] P.G. Jessop, F. Joó, C.C. Tai, *Coord. Chem. Rev.* 248 (2004) 2425–2442.
- [7] R. Tanaka, M. Yamashita, K. Nozaki, *J. Am. Chem. Soc.* 131 (2009) 14168–14169.
- [8] M. Ahlquist, G. Fabrizi, S. Cacchi, P.-O. Norrby, *J. Am. Chem. Soc.* 128 (2006) 12785–12793.
- [9] S.Y. Yang, M.L. Xiang, L.J. Chen, G.B. Xie, B. Shi, Y.Q. Wei, T. Ziegler, *J. Comput. Chem.* 28 (2007) 513–518. We have not located a transition state for the dissociation but not that previous work found that the free energy barrier for ligand dissociation was only slightly higher than the dissociation energy.
- [10] W.N. Olmstead, Z. Margolin, F.G. Bordwell, *J. Org. Chem.* 45 (1980) 3295–3299.
- [11] M.A. Iron, E. Ben-Ari, R. Cohen, D. Milstein, *Dalton Trans.* (2009) 9433–9439.
- [12] E. Ben-Ari, G. Leitus, L.J.W. Shimon, D. Milstein, *J. Am. Chem. Soc.* 128 (2006) 15390–15391.
- [13] A.D. Becke, *J. Chem. Phys.* 98 (1993) 5648–5652.

- [14] C. Lee, W. Yang, R.G. Parr, *Phys. Rev. B* 37 (1988) 785–789.
- [15] Jaguar 7.5 by Schrödinger LLC, Portland OR.
- [16] Y. Zhao, D.G. Truhlar, *Theor. Chem. Acc.* 120 (2006) 215–241.
- [17] J.M.L. Martin, *Chem. Phys. Lett.* 310 (1999) 271–276.
- [18] J.M.L. Martin, A. Sundermann, *J. Chem. Phys.* 114 (2001) 3408–3420.
- [19] D.J. Tannor, B. Marten, R. Murphy, R.A. Friesner, D. Sitkoff, A. Nicholls, M. Rignalda, W.A. Goddard III, B.J. Honig, *J. Am. Chem. Soc.* 116 (1994) 11875–11882.
- [20] B. Marten, K. Kim, C. Cortis, R.A. Friesner, R.B. Murphy, M.N. Rignalda, D. Sitkoff, B. Honig, *J. Phys. Chem.* 100 (1996) 11775–11788.
- [21] C.P. Kelly, C.J. Cramer, D.G. Truhlar, *J. Phys. Chem. B* 110 (2006) 16066–16081.
- [22] A.V. Marenich, R.M. Olson, C.P. Kelly, C.J. Cramer, D.G. Truhlar, *J. Chem. Theory Comput.* 3 (2007) 2011–2033.
- [23] M. Ahlquist, S. Kozuch, S. Shaik, D. Tanner, P.-O. Norrby, *Organometallics* 25 (2006) 45–47.
- [24] J.A. Keith, R.J. Nielsen, J. Oxgaard, W.A. Goddard III, *J. Am. Chem. Soc.* 129 (2007) 12342–12343.